Biocatalysis

Deutsche Ausgabe: DOI: 10.1002/ange.201913686
Internationale Ausgabe: DOI: 10.1002/anie.201913686

Control of Stereoselectivity in Diverse Hapalindole Metabolites is Mediated by Cofactor-Induced Combinatorial Pairing of Stig Cyclases**

*Shasha Li, Sean A. Newmister, Andrew N. Lowell, Jiachen Zi, Callie R. Chappell, Fengan Yu, Robert M. Hohlman, Jimmy Orjala, Robert M. Williams und David H. Sherman**

Abstract: *Stereospecific polycyclic core formation of hapalindoles and fischerindoles is controlled by Stig cyclases through a three-step cascade involving Cope rearrangement, 6-exo-trig cyclization, and a final electrophilic aromatic substitution. Reported here is a comprehensive study of all currently annotated Stig cyclases, revealing that these proteins can assemble into heteromeric complexes, induced by Ca^{2+}, to cooperatively control the stereochemistry of hapalindole natural products.*

Introduction

After many years of isolation, structural characterization, and total synthesis,[1] hapalindole-type alkaloids from Stigonematales cyanobacteria have regained significant scientific attention because of their pharmacological potential and unique biogenesis. Recent studies have revealed that hapalindole H (**4a**; see Figure 1) inhibits NF-κB and has selective cytotoxicity against the PC-3 prostate cancer cell line,[2] while 12-*epi*-hapalindole H (**5a**) shows embryo toxicity in vertebrate development.[3] Several other hapalindoles appear to be neurotoxins by modulating sodium channels in human cells.[4] A growing focus of several research groups involves the elucidation of the biosynthetic mechanism of these alkaloids,[5] specifically their stereo- and regiochemically diverse polycyclic ring formation,[6] which results in six stereochemical patterns based on the C10, C11, C12, and C15 chiral centers (Figure 1). We recently reported a novel class of Stig cyclases that specify hapalindole and fischerindole formation from the central C3-geranylated *cis*-indole isonitrile intermediate (**1**, Figure 1; see Figure S1 in the Supporting Information).[5a] This class of enzyme catalyzes a Cope rearrangement/ring-forming cascade and elaborates the four chiral centers and three types of ring systems.[6a] Considerable recent progress has been made toward a mechanistic understanding of these core assembly reactions through a crystal structure of the HpiC1 cyclase and computational modeling of the three-part reaction scheme.[7] However, further studies of these remarkable biocatalysts are required to fully understand the basis for stereochemical control during assembly of diverse hapalindole and fischerindole metabolites.

In a previous report,[6a] we characterized several Stig cyclases, including FamC1 and its homologues FilC1/HpiC1, which generate 12-*epi*-hapalindole U (**3a**), FimC5/FisC generating 12-*epi*-fischerindole U (**3c**), and the heterodimeric combination FamC2-FamC3 generating hapalindole H (**4a**; Figure 1). Phylogenetic analysis was applied to predict the product profile of Stig cyclases based on the rationale that proteins with high sequence identity will produce the same or highly similar metabolites.[6a] In addition, we demonstrated that Stig cyclases function as homodimeric (e.g. FamC1) or heterodimeric (e.g. FamC2-FamC3) complexes to generate stereochemically distinct products. These results provided an initial characterization of the stereoselectivity and regioselective divergence for C-ring coupling between hapalindoles and fischerindoles.

In the current study, we sought to decrypt the basis for stereoselectivity among all six naturally observed stereochemical patterns identified from over 30 years of studies involving direct isolation of metabolites from wild-type cyanobacterial strains.[1b,3] These studies provide a new, nuanced biochemical understanding of the Stig cyclases, and reveal a natural system for combinatorial biocatalytic diversification in these pathways.

[*] Prof. D. H. Sherman
Life Sciences Institute, Departments of Medicinal Chemistry, Chemistry, Microbiology & Immunology
The University of Michigan
210 Washtenaw Avenue, Ann Arbor, MI 48109-2216n (USA)
E-Mail: davidhs@umich.edu
Dr. S. Li, R. M. Hohlman
Life Sciences Institute, Department of Medicinal Chemistry
The University of Michigan (USA)
Dr. S. A. Newmister, Dr. A. N. Lowell, Dr. F. Yu
Life Science Institute, The University of Michigan (USA)
C. R. Chappell
Department of Molecular, Cellular & Developmental Biology
The University of Michigan (USA)
Dr. J. Zi, Prof. J. Orjala
Department of Pharmaceutical Sciences, College of Pharmacy, University of Illinois at Chicago, Chicago, IL 60612 (USA)
Prof. R. M. Williams
Department of Chemistry, Colorado State University
Fort Collins, CO 80523 (USA)
and
University of Colorado Cancer Center
Aurora, CO 80045 (USA)
Dr. A. N. Lowell
Department of Chemistry, Virginia Tech Blacksburg VA 24061 (USA)

[**] A previous version of this manuscript has been deposited on a preprint server (https://doi.org/10.26434/chemrxiv.10032260.v1).

Supporting information and the ORCID identification number(s) for the author(s) of this article can be found under: https://doi.org/10.1002/anie.201913686.

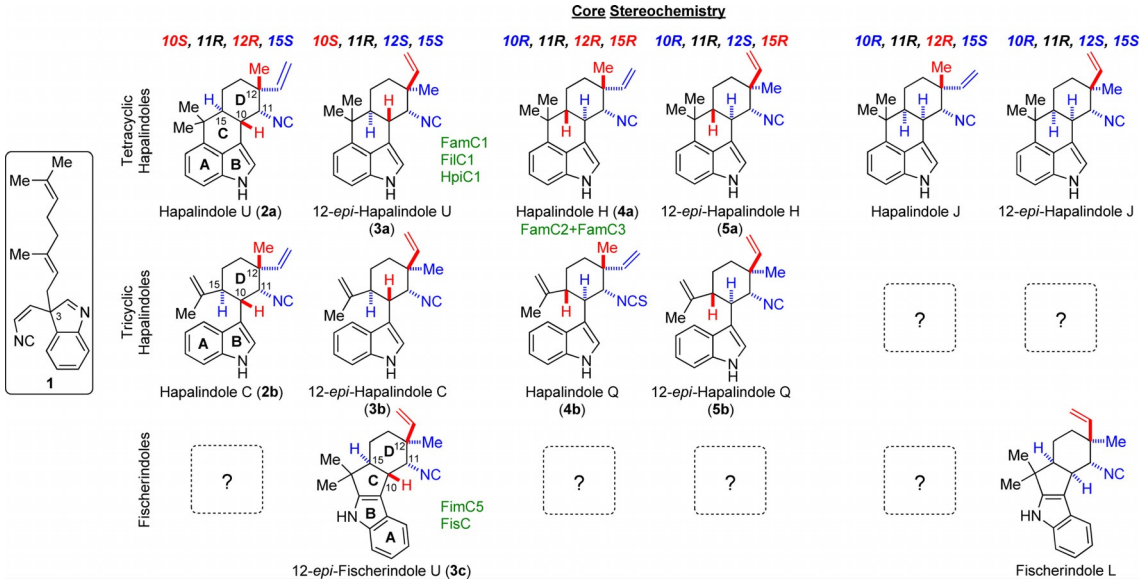

Figure 1. Stereochemical classification of hapalindole and fischerindole metabolites based on C10, C11, C12, and C15 stereocenters. All chemical patterns were discovered from nature, except 12-*epi*-hapalindole U (**3a**) which was initially identified from in vitro chemoenzymatic assay.[5a] However, its stereo-pattern has been observed in 12-*epi*-ambiguine B nitrile.[3] Dashed-line boxes with a question mark represent stereochemical configurations that are predicted, but remain unidentified as isolated natural products. The characterized Stig cyclases are shown adjacent its (major) products (green text).

Results and Discussion

The course of our studies described here was developed upon noticing a mismatch in reported metabolites from the ambiguine-producing strain *Fischerella* sp. IL 199-3-1 (*fil*),[8] and product prediction from its Stig cyclases based on phylogenetic analysis. The *fil* gene cluster contains four Stig cyclases (FilC1–FilC4), which share high sequence similarities to FamC1–FamC4 from *Fischerella ambigua* UTEX 1903. We demonstrated previously that FilC1 is a FamC1 functional homologue and catalyzes formation of **3a** (Figure 2).[6a] While both FilC2 and FilC3 are 98% identical to FamC2 and FamC3, respectively, they were expected to produce **4a**. However, the isolated metabolites from cultured *Fischerella* sp. IL 199-3-1 contains 12-*epi*-hapalindole H (**5a**; C10*R*, 11*R*, 12*S*, and 15*R*) instead of **4a** (C10*R*, 11*R*, 12*R*, and 15*R*; see Figure S2).[8,9] Because of this discordance with expectations, we decided to address whether FilC2-FilC3 behaves differently from FamC2-FamC3 to produce **5a** instead of **4a** despite such high sequence identities. Thus, we generated FilC2 and FilC3 in *E. coli* and analyzed the products of the in vitro reaction.

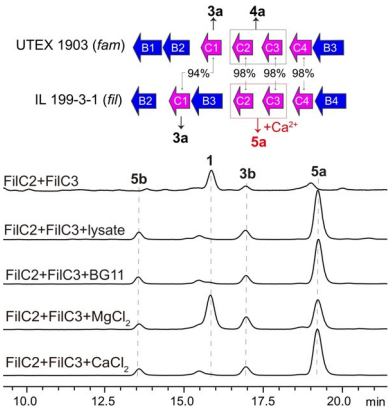

Figure 2. FilC2 and FilC3 functional assay with excess calcium (5 mM) leading to 12-*epi*-hapalindole H (**5a**). [Note: all reactions in this report were conducted with 5 mM of calcium chloride unless otherwise noted.].

In this experimental system, FilC2 and FilC3 were almost completely inactive both as a pair and as individual proteins, in contrast to FamC2 and FamC3, which together produce **4a** in a heterodimeric form.[6a] Based on our hypothesis that a missing cellular component was required for activity, the cell-free lysate of *Fischerella sp.* IL 199-3-1 was introduced into the reaction mixture and facile conversion of **1** was observed (Figure 2). Furthermore, we found that the BG-11 culture broth alone, a metal-rich medium used for cyanobacterial cultivation, is sufficient to stimulate the activity. Additional screening with the metal components in the BG-11 broth revealed that supplemental calcium chloride and magnesium chloride promoted the reaction, with Ca^{2+} exhibiting the highest efficiency (Figure 2; see Figure S4). To characterize the structure of the FilC2-FilC3 derived metabolites, we conducted a large-scale in vitro reaction using **1** with 5 mM of $CaCl_2$ and isolated the products for NMR analysis. Under these conditions, the major compound was identified as **5a** (see Figure S5 and Table S3), which is consistent with its isolation from cultured *Fischerella sp.* IL 199-3-1.[8] Thus, we confirmed that despite FilC2/FilC3 being 98% identical to the FamC2/FamC3 system, the metabolite **5a**, having an alternative C12 stereochemistry (compared to **4a**),[6a,9b] was produced. Minor products were also isolated, two of which we identified as tricyclic variants 12-*epi*-

hapalindole C (**3b**)[6a] and 12-*epi*-hapalindole Q (**5b**; see Figure S6).[10]

The FilC2-FilC3 pair was the first example in our investigation that required excess Ca^{2+} for function and resulted in formation of different metabolites compared to their most closely related Stig cyclase homologues. To assess the effect of Ca^{2+} on metabolite stereochemical configuration, we compared the products of FamC2-FamC3 and other previously characterized Stig cyclases[6a] after introduction of excess Ca^{2+}, and found that these metabolite profiles remained unchanged. While all reactions could be suppressed by adding EDTA, we confirmed that Ca^{2+} is a key component for functional Stig cyclases. In addition to maintaining structural and functional integrity,[7a] it is now evident that excess Ca^{2+} plays another important role in FilC2-FilC3, a realization that motivated further detailed studies.

We proceeded by testing individual Stig cyclases with excess Ca^{2+} and found that it activates FilC2 to produce the same metabolites observed when paired with FilC3, albeit at reduced levels. By contrast, even with excess Ca^{2+}, FilC3 and FamC3 remained catalytically inactive in the absence of FilC2 and FamC2, respectively. Surprisingly, FamC2 alone generated **5a** instead of **4a**, the product of heterodimeric FamC2-FamC3 (Figure 3; see Figure S7). This observation compelled us to reconsider the role of FamC3 in controlling the stereochemistry at C12 during hapalindole assembly. Based on the high degree of similarity between FamC3 and FilC3, we decided to investigate the heterologous cross-pairing of FamC2-FamC3 and FilC2-FilC3 (Figure 3). We found that pairing of FamC2-FilC3 resulted in production of **5a**, identical to the product obtained with FamC2 alone. However, pairing of FilC2-FamC3 resulted in formation of **4a**, different from FilC2-FilC3, which was further shown by ^{1}H NMR analysis to be a 4:1 mixture of **4a** and **5a** (see Figure S8). Two of the three minor products were confirmed to be tricyclic hapalindole C (**2b**; see Figure S9) and **3b**. Similar results were observed in another homologous pair HpiC2 (99% identical to FamC2) and HpiC3 (100% identical to FamC3 of the first 198/202 amino acids),[6a] where HpiC3 can modulate the reaction outcome from the expected **5a** of HpiC2/FamC2 to **4a** (see Figure S10). This result suggests that FamC3/HpiC3 may actively control the stereochemistry of hapalindoles, while FilC3 does not exert similar control.

This product profile reconfiguration was also observed in our investigation of another hapalindole/ambiguine-producing strain, *Westiellopsis prolifica* SAG 16.93 (*wep*), which also showed a discrepancy between metabolites isolated from the cyanobacterium, and products predicted from Stig cyclase sequence comparisons. This strain is known to produce **2a** and **4a** (see Figure S3), but only two Stig cyclases were identified in the *wep* gene cluster, denoted as WepC1 and WepC2. WepC1 was classified as a FamC1 homologue based on 89% sequence identity, while WepC2 is a FamC4 homologue with 93% identity. Despite observed production of **4a** by this strain, no FamC2/FamC3 homologues were identified from the *wep* cluster or from analysis of the broader genome sequence (Figure 4). In vitro assays demonstrated that WepC1 behaves similarly to FamC1 by producing **3a** as the major metabolite, in addition to low levels of the tricyclic **3b** (10%). WepC1 differs from FamC1 in that it requires excess Ca^{2+} for activity. WepC2 was inactive (similar to FamC4), both with and without excess calcium. Thus, after analyzing both cyclases individually, neither of them generated the hapalindoles isolated from *W. prolifica* SAG 16.93. Inspired by our finding with FilC2-FilC3, we combined WepC1 and WepC2 in a 1:1 ratio with 5 mM of $CaCl_2$, and the product profile was completely altered. Instead of **3a**, the WepC1-WepC2 heteromeric combination produced three new metabolites (Figure 4), characterized through NMR analysis to be **2a** (C10*S*, 11*R*, 12*R*, and 15*S*), **2b** (5:1 ratio; see Figure S11), and trace levels of **4a**.

The discovery of product profile reconfiguration induced by heteromeric pairing of Stig cyclases inspired us to track the **2a** producer. Except the 12-*epi*-ambiguine nitrile,[3] all other

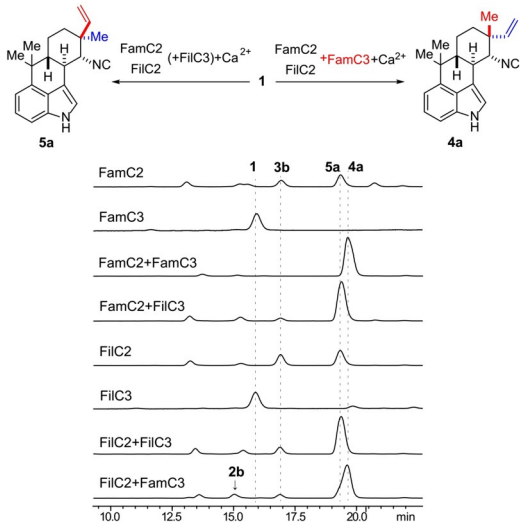

Figure 3. In vitro analysis of FamC2/FamC3, FilC2/FilC3 and their heterologous cross-pairing, with 5 mM $CaCl_2$.

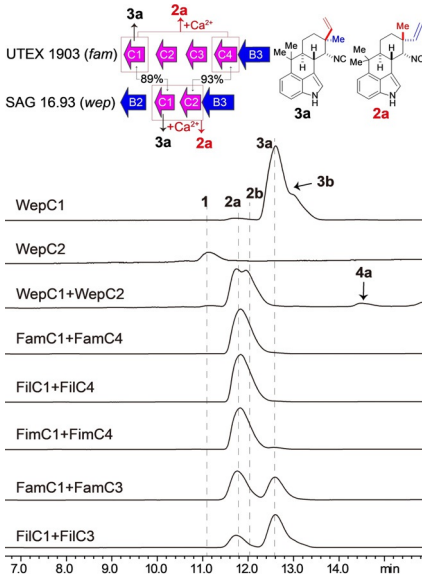

Figure 4. In vitro analysis of WepC1 and WepC2 and homologues for production of hapalindole U (**2a**) with 5 mM $CaCl_2$.

isolated ambiguines share the same stereochemical pattern with **2a** (C10*S*, 11*R*, 12*R*, and 15*S*), which is likely to be the common precursor to ambiguines. In the ambiguine-producing strain *F. ambigua* UTEX 1903, FamC1 is known to generate **3a**.[5a] It is important to note that Dethe and coworkers recently reported the structure of synthetic (−)-12-*epi*-hapalindole U,[11] and our optical rotation of (+)-8.3 is consistent with the stereochemistry of natural product **3a** as C10*S*, 11*R*, 12*S*, and 15*S*. As expected, the product of FamC1 was reconfigured to **2a** by adding FamC4 (Figure 4). Identical results were observed with homologues FilC1-FilC4 and FimC1-FimC4. Moreover, further screening in cyclase cross-pairing experiments revealed that FamC3/FilC3 can also alter the product of FamC1/FilC1 to **2a**, albeit with lower efficiency than FamC4/FilC4 (Figure 4). Notably, the stereochemical alteration only occurred in the presence of excess Ca^{2+} (see Figure S12). We note that production of **2a** was independently reported by Liu et al.[6b] upon combining FamC1 with 10 equivalents of FamC4 and 20 mM $CaCl_2$. Our titration study revealed that 0.5 mM $CaCl_2$ is sufficient to either fully activate 10 μM of Stig cyclase or alter product configuration in heterologous combinations of Fam cyclases (see Figure S13).

In these two cases, we observed a distinct alteration in stereochemistry by adding another cyclase. FamC3, FamC4, and their homologues were initially observed to be cognate partners that appeared to be inactive independently. However, we further reasoned that the active sites of both cyclases may be engaged to cooperatively control hapalindole stereochemistry. To evaluate this hypothesis, we decided to prepare mutants, and compare Stig cyclase activity when one partner of a heterodimeric pair was catalytically inactivated by site-directed mutagenesis.[7a]

In our recent structural study of HpiC1, we probed the critical role of D214, an amino acid residue that is 100% conserved across all identified Stig cyclases and is the likely basis for acid-catalyzed Cope rearrangement (see Figure S3).[7a] By mutating this residue, HpiC1 activity was completely abrogated. Accordingly, this conserved residue was mutated to alanine, (FamC1-D214A, FamC2-D217A, FamC3-D214A, and FamC4-D215A), and each variant enzyme was confirmed to be inactive in the in vitro assay either as an individual cyclase or heterodimeric pair (see Figure S14). Functional activity of the FamC3-D214A mutant was analyzed by incubating with wild-type FamC2 or FilC2 (Figure 5). We found that the catalytically inactive FamC3 mutant was no longer able to alter the product profiles; resulting in production of **5a** in both cases. Indeed, this is the same product obtained when an individual FamC2 or FilC2 enzyme is employed. Moreover, no alkaloid products were obtained when FamC2-D217A was combined with FamC3-wild-type or FamC3-D214A, indicating that FamC2 mediates an indispensable part of the catalytic reaction to form hapalindoles (see Figure S14). Comparable results were obtained with mutants FamC1-D214A and FamC4-D215A, with reactions including FamC1-D214A failing to generate a product, while reaction with FamC1-wild-type and FamC4-D215A yielded **3a** (Figure 5). Concordant results were observed with homologues WepC1-D214A and WepC2-D215A (see Figure S14).

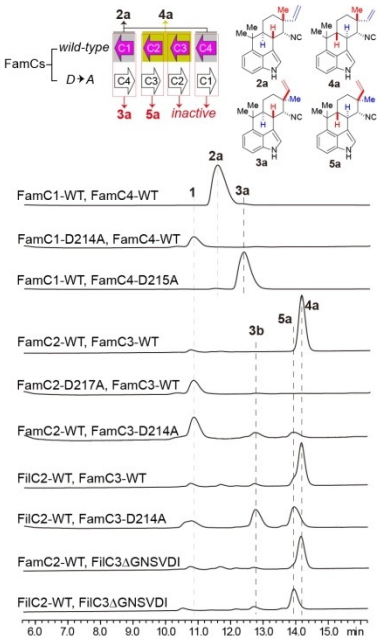

Figure 5. In vitro reactions of FamC1, FamC2, FamC3, FamC4, and select mutants with substrate **1** using 5 mM $CaCl_2$.

The experimental data described above are consistent with the hypothesis that a functional active site in FamC3 and FamC4 is required to cooperatively control the C12 stereochemistry of hapalindoles. This insight also serves to identify the difference between FilC3 and FamC3, that despite sharing 98% identity with FamC3, FilC3 contains a six amino-acid insertion (NSVDIG) proximal to the active site, which is likely to alter the active-site architecture (see Figure S15), and thus influencing cyclase catalytic activity. We mutated FilC3 by deleting the extra six residues, and the enzymatic assay supported our hypothesis that FilC3ΔNSVDIG re-established its ability to alter FamC2 for production of **4a**. But interestingly, it did not change the product of FilC2 (Figure 3 and Figure 5).

These data further support our hypothesis that FamC3, FamC4, and their homologues are engaged in hapalindole biosynthesis as subunits that combine for substrate catalysis in the Stig cyclase heteromeric pair. Interestingly, the products from the heteromeric pairs, **2a** (FamC1-FamC4) and **4a** (FamC2-FamC3), are reported natural metabolites from *F. ambigua* UTEX 1903. Thus, it is reasonable to conclude that such combinatorial pairing of Stig cyclases is biologically relevant to the intracellular environment. Another intriguing observation regarding the reconfiguration is that either **3a** (10*S*, 11*R*, 12*S*, 15*S*) to **2a** (10*S*, 11*R*, 12*R*, 15*S*), or **5a** (10*R*, 11*R*, 12*S*, 15*R*) to **4a** (10*R*, 11*R*, 12*R*, 15*R*) show alteration at the C12 chiral center only, which is established during the Cope rearrangement step (Figure 6). The C10 and C15 chiral centers installed in the 6-*exo*-trig cyclization remain intact, along with the C-ring regiochemistry determined during terminal electrophilic aromatic substitution. A similar pattern was observed in the WepC1-WepC2 pair with a product change from **3a** + **3b** to **2a** + **2b**. These data suggest that the Cope rearrangement is singularly affected in the heteromeric

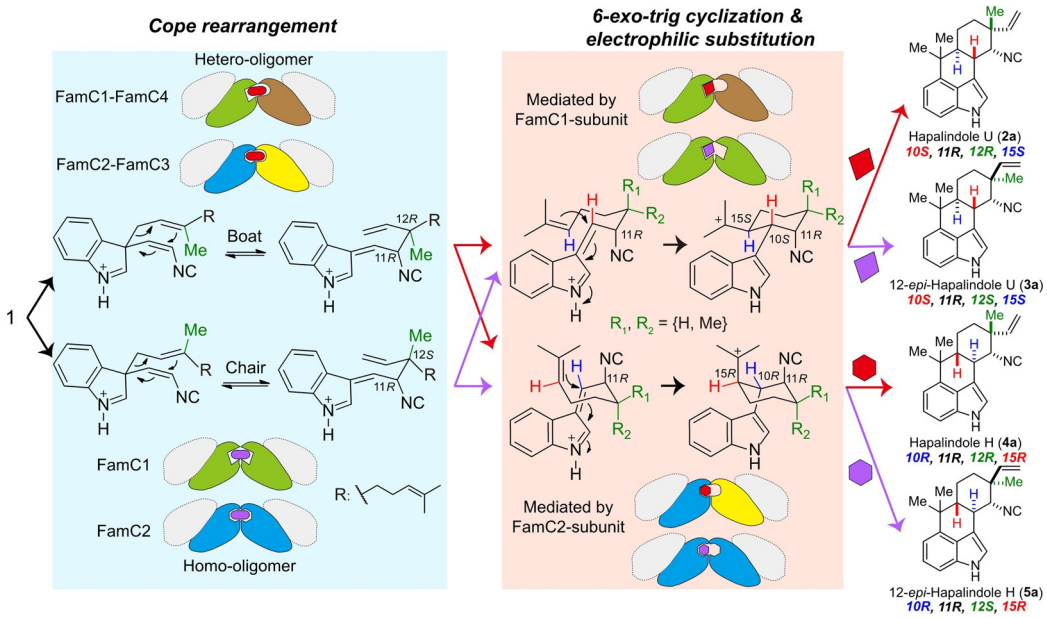

Figure 6. Proposed oligomeric model to form a combined cyclase active site for control of hapalindole stereochemistry. In this model, Cope rearrangement of **1** is catalyzed by a combined active site to generate the C11 and C12 stereochemical pattern either by a boat conformation [hetero-oligomer FamC1-FamC4 (monomer is shown in green/khaki)] and FamC2-FamC3 (cyan/yellow) or by a chair conformation (homo-oligomer FamC1 and FamC2). The substrate is displayed as a red (boat; 12*R*) or purple (chair; 12*S*) oval in the combined active site. Both intermediates are transferred to the primary subunit (FamC1 or FamC2) to conduct the 6-*exo*-trig cyclization, where the oligomer comprising a FamC1-subunit (hetero-FamC1-FamC4 or homo-FamC1) generates the 10*S*/15*S* stereochemical pattern (diamond shape), while FamC2 forms 10*R*/15*R* (hexagon shape). Thus, four final intermediates are poised for the final electrophilic aromatic substitution to generate four products (**2a**/**3a**/**4a**/**5a**). We show a white monomer surrounded by a dashed-line in each dimeric substructure to denote that the nature of the putative oligomeric cyclase structure (derived from homodimer or heterodimer) remains unknown.

Stig cyclase combinations. The 6-*exo*-trig cyclization and subsequent electrophilic aromatic substitution (or deprotonation to generate the tricyclic hapalindoles) are controlled by the independently active FamC1 and FamC2 and their homologues, which may be considered primary biocatalytic subunits as they are capable of functioning independently (Figure 6).

Currently, we have demonstrated the importance of FamC3, FamC4, and their Stig cyclase homologues for control (with their cognate cyclase partners) of stereochemical induction during biogenesis of hapalindole core molecules. The precise molecular interactions involved to generate each of the known stereo- and regiochemical outcomes remains to be examined. Recent studies established the homodimeric conformation of HpiC1 by X-ray analysis,[7a,b] and biochemical evidence supports formation of Stig cyclase heterodimers, such as FamC2-FamC3.[6a] Based on the HpiC1 crystal structure and the high sequence homology of all Stig cyclases, we can deduce that the two active sites are too distant for a viable interaction in the dimeric state. Furthermore, based on the active-site position and protein characteristics, we do not anticipate that a transient post-Cope intermediate could be readily transferred between distal active sites.[7a] However, if a higher-order oligomer with at least two dimers is generated, an arrangement involving a joint active site derived from two distinct Stig cyclase subunits could be achieved (Figure 6).[12]

In our earlier studies, we observed that HpiC1 cannot produce **2a** by pairing with HpiC4 or any other HpiC proteins, in contrast to FamC1-FamC4 (Figure 7). Moreover, we previously observed a form of HpiC1 with alternative crystal packing comprising a protein interface where the adjoining cyclase active sites are in direct contact (see Figure S16). In this form bridging Ca^{2+} ions were observed at the interface, suggesting that higher-order oligomerization

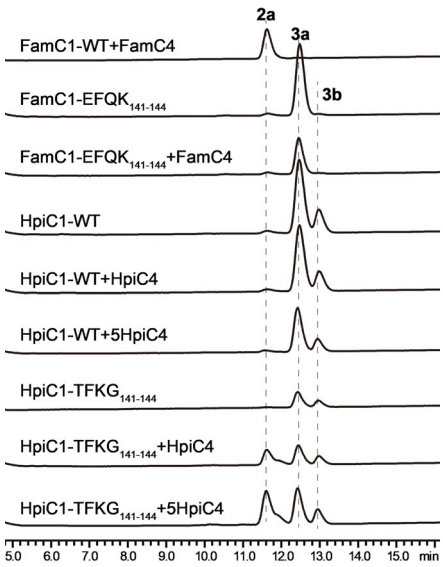

Figure 7. In vitro assay of FamC1 and HpiC1 mutants with substrate **1** and 5 mM of $CaCl_2$.

could be influenced by Ca^{2+}.[7a] We further found that in the proposed oligomer interface (residues 141–144), HpiC1 has different residues (EFQK) than FamC1 (TFKG), while both HpiC4 and FamC4 possess SKDI residues (see Figure S16). We hypothesized that this disparity results in a variant oligomer form and active-site interaction between HpiC1 and FamC1. To probe this hypothesis further we generated two mutants, HpiC1-$TFKG_{141\text{-}144}$ and FamC1-$EFQK_{141\text{-}144}$, to interchange their activities by exchanging these corresponding interface residues. The enzymatic assay showed that FamC1- $EFQK_{141\text{-}144}$ failed to generate **2a** by pairing with FamC4, while HpiC1-$TFKG_{141\text{-}144}$ gained the ability to produce **2a** by interacting with HpiC4 (Figure 7). These results support our mechanistic hypothesis that Stig cyclases may function through formation of higher-order oligomeric states.

Further work is still necessary to validate this hypothesis, as the FamC2-FamC3 hetero-oligomer and FamC1 homodimer do not require supplemental Ca^{2+} to function. In contrast, as shown above, the FamC1-FamC4 hetero-oligomer and WepC1 homodimer require excess levels of calcium. Taken together, these data indicate that the integrity of both active sites in the heteromeric cyclase associations is required to affect the stereochemical outcome of the Cope rearrangement, and the role of calcium in this process appears to be twofold. First, with two integral sites in each protein subunit, Ca^{2+} is required for structural integrity and activity of Stig cyclases based on the HpiC1[7a] and FamC1[7b] crystal structure (and abrogation of activity by EDTA). Second, calcium appears to also play a role in functional heteromeric or homo-oligomeric complexes to enable formation of a combined Stig cyclase active sites with resulting control of chiral induction at C12 during the Cope rearrangement.

Conclusion

In this study, we initially explored the enzymatic activity of the Stig cyclases FilC2 and FilC3 to produce **5a**, which led to the discovery of Ca^{2+} as an important co-factor for functional Stig cyclases. Further interrogation with homologues FamC2 and FamC3 demonstrated that the product of FamC2 alone is **5a**. However, when FamC2 is combined with FamC3 the heteromeric complex specifically generates **4a**. This unexpected catalytic function of FamC3 was further observed in FamC4 (and its homologues FamC4/WepC2/FilC4/FimC4). In this case, the original **3a** metabolite of FamC1/WepC1/FilC1/FimC1 can be redirected to **2a** when combined with its cognate partner and supplemental (5 mM) $CaCl_2$. Mutational analysis of the active-site residue (D214A) with FamC cyclases and FilC3ΔNSVDIG supported our hypothesis that FamC3, FamC4, and their homologues are cooperating to control the stereochemistry of hapalindole products through Ca^{2+}-promoted heteromeric pairing with cognate Stig cyclases. These biochemical observations are consistent with our recent HpiC1 crystal structure analysis that revealed Stig cyclases form higher-order oligomers, and are further reinforced by mutagenesis studies on FamC1 and HpiC1. Taken together, these functional and structural data provide a new proposal for stereocontrol in Stig cyclases. Our data indicate that as a first step, the Cope rearrangement is mediated by a combined active site comprising heteromeric cyclase complexes. Next, the Cope rearrangement product shifts to the dominant cyclase monomer to complete the 6-*exo-trig* cyclization and C-ring formation (Figure 6). Further structural and biochemical studies are in progress to verify the hetero-oligomeric complex formation and characterize additional stereochemical patterns (such as hapalindole J, and other predicted, but unidentified hapalindole/fischerindole metabolites; Figure 1) mediated by Stig cyclase biocatalysts.

Acknowledgements

The authors thank the National Institutes of Health for financial support (R35 GM118101) as well as the National Science Foundation under the CCI Center for Selective C–H Functionalization (CHE- 1700982), and the Hans W. Vahlteich Professorship (to DHS). JO (UIC) thanks P01 CA125066 for supporting research on *Westiellopsis prolifica* SAG 16.93.

Conflict of interest

The authors declare no conflict of interest.

Stichwörter: Biokatalyse · Cyclasen · Indole · Oligomerisierung · Umlagerungen

Zitierweise: *Angew. Chem. Int. Ed.* **2020**, *59*, 8166–8172
Angew. Chem. **2020**, *132*, 8243–8249

[1] a) R. E. Moore, C. Cheuk, G. M. L. Patterson, *J. Am. Chem. Soc.* **1984**, *106*, 6456–6457; b) V. Bhat, A. Dave, J. A. MacKay, V. H. Rawal, in *The Alkaloids: Chemistry and Biology*, *Vol. 73* (Ed.: K. Hans-Joachim), Academic Press, San Diego, **2014**, pp. 65–160.

[2] U. M. Acuña, S. Mo, J. Zi, J. Orjala, E. J. C. De Blanco, *Anticancer Res.* **2018**, *38*, 3299–3307.

[3] K. Walton, M. Gantar, P. Gibbs, M. Schmale, J. Berry, *Toxins* **2014**, *6*, 3568–3581.

[4] E. Cagide, P. G. Becher, M. C. Louzao, B. Espiña, M. R. Vieytes, F. Jüttner, L. M. Botana, *Chem. Res. Toxicol.* **2014**, *27*, 1696–1706.

[5] a) S. Li, A. N. Lowell, F. Yu, A. Raveh, S. A. Newmister, N. Bair, J. M. Schaub, R. M. Williams, D. H. Sherman, *J. Am. Chem. Soc.* **2015**, *137*, 15366–15369; b) M. L. Hillwig, Q. Zhu, X. Liu, *ACS Chem. Biol.* **2014**, *9*, 372–377; c) M. L. Micallef, D. Sharma, B. M. Bunn, L. Gerwick, R. Viswanathan, M. C. Moffitt, *BMC Microbiol.* **2014**, *14*, 213–230; d) M. L. Hillwig, H. A. Fuhrman, K. Ittiamornkul, T. J. Sevco, D. H. Kwak, X. Liu, *ChemBioChem* **2014**, *15*, 665–669.

[6] a) S. Li, A. N. Lowell, S. A. Newmister, F. Yu, R. M. Williams, D. H. Sherman, *Nat. Chem. Biol.* **2017**, *13*, 467–469; b) Q. Zhu, X. Liu, *Angew. Chem. Int. Ed.* **2017**, *56*, 9062–9066; *Angew. Chem.* **2017**, *129*, 9190–9194.

[7] a) S. A. Newmister, S. Li, M. Garcia-Borràs, J. N. Sanders, S. Yang, A. N. Lowell, F. Yu, J. L. Smith, R. M. Williams, K. N. Houk, D. H. Sherman, *Nat. Chem. Biol.* **2018**, *14*, 345–351; b) C. C. Chen, X. Hu, X. Tang, Y. Yang, T. P. Ko, J. Gao, Y. Zheng, J. W. Huang, Z. Yu, L. Li, S. Han, N. Cai, Y. Zhang, W.

Liu, R. T. Guo, *Angew. Chem. Int. Ed.* **2018**, *57*, 15060 – 15064; *Angew. Chem.* **2018**, *130*, 15280 – 15284; c) X. Tang, J. Xue, Y. Yang, T.-P. Ko, C.-Y. Chen, L. Dai, R.-T. Guo, Y. Zhang, C.-C. Chen, *RSC Adv.* **2019**, *9*, 13182 – 13185.

[8] A. Raveh, S. Carmeli, *J. Nat. Prod.* **2007**, *70*, 196 – 201.

[9] a) T. A. Smitka, R. Bonjouklian, L. Doolin, N. D. Jones, J. B. Deeter, W. Y. Yoshida, M. R. Prinsep, R. E. Moore, G. M. L. Patterson, *J. Org. Chem.* **1992**, *57*, 857 – 861; b) S. Mo, A. Krunic, G. Chlipala, J. Orjala, *J. Nat. Prod.* **2009**, *72*, 894 – 899.

[10] a) Z. Lu, M. Yang, P. Chen, X. Xiong, A. Li, *Angew. Chem. Int. Ed.* **2014**, *53*, 13840 – 13844; *Angew. Chem.* **2014**, *126*, 14060 – 14064; b) D. Klein, D. Daloze, J. C. Braekman, L. Hoffmann, V. Demoulin, *J. Nat. Prod.* **1995**, *58*, 1781 – 1785; c) T. J. Maimone, Y. Ishihara, P. S. Baran, *Tetrahedron* **2015**, *71*, 3652 – 3665.

[11] D. H. Dethe, S. Das, V. B. Kumar, N. A. Mir, *Chem. Eur. J.* **2018**, *24*, 8980 – 8984.

[12] a) J. Vonck, D. J. Mills, *Curr. Opin. Struct. Biol.* **2017**, *46*, 48 – 54; b) V. Villeret, B. Clantin, C. Tricot, C. Legrain, M. Roovers, V. Stalon, N. Glansdorff, J. Van Beeumen, *Proc. Natl. Acad. Sci. USA* **1998**, *95*, 2801 – 2806.

Manuskript erhalten: 27. Oktober 2019
Akzeptierte Fassung online: 13. Februar 2020
Endgültige Fassung online: 19. März 2020

